

Predictive Voltage Control of Transformerless Dynamic Voltage Restorer

Chandan Kumar, *Student Member, IEEE*, and Mahesh K. Mishra, *Senior Member, IEEE*

Abstract—This paper presents a predictive voltage control scheme for the effective control of a transformerless dynamic voltage restorer (TDVR). This control scheme utilizes the discrete model of a voltage source inverter and an interfacing filter for the generation of the switching strategy of inverter switches. Predictive voltage control algorithm-based TDVR tracks the reference voltage effectively and maintains load voltages sinusoidal during various voltage disturbances as well as load conditions. Moreover, this scheme does not require any linear controller or modulation technique. Simulation and experimental results are presented to verify the performance of the proposed scheme.

Index Terms—Predictive voltage control, transformerless dynamic voltage restorer (DVR) (TDVR), voltage disturbance.

I. INTRODUCTION

VOLTAGE disturbances such as sag, swell, unbalance, and/or transients have adverse effects on sensitive loads [1], [2]. The dynamic voltage restorer (DVR), one of the custom power devices, has been utilized to protect sensitive loads from these voltage disturbances [3]–[6]. The DVR injects a compensating voltage in series with the line through an injection transformer to maintain the load voltage at a desired value. However, several issues, namely, cost, weight, and losses related with the series injection transformer, make the application of conventional DVR undesirable at places like homes, offices, etc. To overcome these limitations of the conventional DVR, a transformerless DVR (TDVR) scheme with reduced cost, weight, size, and losses has been proposed [7], [8]. The TDVR satisfactorily mitigates the voltage disturbances and maintains a constant voltage at the load terminal.

Generally, pulsewidth-modulation technique, hysteresis controller, sliding-mode controller, etc., are used to control the switches of the voltage source inverter (VSI) [9]. Recently, a predictive control scheme has found applications in the control of power electronic converters such as single-phase and three-phase VSIs, rectifiers, active power filters, uninterrupted power supplies, dc–dc converters, and motor drive [10]–[19]. Increasing interest in predictive control schemes over other controllers

Manuscript received April 6, 2014; revised June 16, 2014, August 7, 2014, and September 25, 2014; accepted October 14, 2014. Date of publication October 29, 2014; date of current version April 8, 2015. This work was supported by the Department of Science and Technology, India, under Grant DST/TM/SERI/2k10/47(G).

The authors are with the Department of Electrical Engineering, Indian Institute of Technology Madras, Chennai 600 036, India (e-mail: chandan3107@gmail.com; mahesh@ee.iitm.ac.in).

Color versions of one or more of the figures in this paper are available online at <http://ieeexplore.ieee.org>.

Digital Object Identifier 10.1109/TIE.2014.2365753

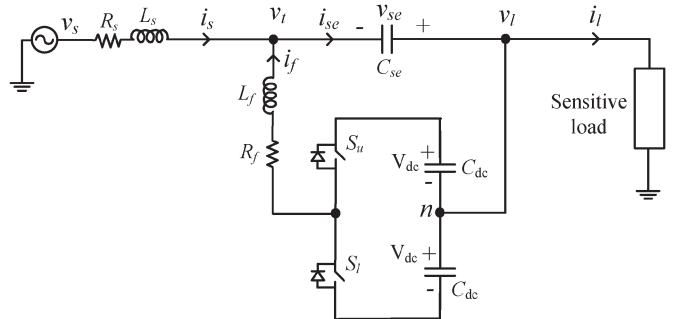


Fig. 1. Single-phase TDVR compensated distribution system.

is due to the fact that the scheme is easy to implement in modern digital signal processor (DSP), has fast dynamic response, and does not require any modulator. Moreover, system nonlinearities and necessary constraints can be easily accommodated in the control scheme.

This paper presents a predictive voltage control scheme for TDVR to maintain load voltage at a constant value during voltage disturbance as well as under unbalanced and nonlinear loads. A detailed discrete-time state-space model of the TDVR compensated system is derived to predict the future values of the load voltage, which depends upon the sensed currents and voltages. A cost function is chosen for the selection of the appropriate switching state such that the square of error between the actual and reference voltages is minimized. Simulation and experimental results confirm the feasibility and usefulness of the proposed scheme.

II. MODELING OF TDVR COMPENSATED SYSTEM

A. Description of System

The power circuit diagram of the single-phase TDVR compensated system used in this work is shown in Fig. 1 [7], [8]. The source voltage is represented by v_s . The resistance and inductance of the source are R_s and L_s , respectively. The source, load, filter, and series capacitor currents are represented by i_s , i_l , i_f , and i_{se} , respectively. The source is supplying to an unbalanced nonlinear load. The TDVR consists of a half-bridge VSI, an output filter (L_f and C_{se}), and neutral-point-clamped dc capacitors. The voltage across the filter capacitor (v_{se}) connected in series with the line is controlled to maintain the desired voltage at the load point.

The equivalent circuit of the TDVR at any time of operation is shown in Fig. 2. The term u is the switching variable. The upper and lower switches, S_u and S_l , respectively, are operated in a complementary way, i.e., if the upper switch is ON ($u = 1$) then the lower switch will be OFF ($u = -1$) at any time instant and vice versa. A voltage of V_{dc} is maintained across each of the

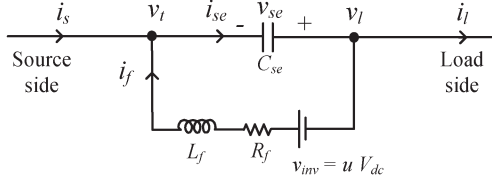


Fig. 2. Equivalent circuit of TDVR in distribution system.

dc-link capacitor \$C_{dc}\$. A voltage of \$v_{se}\$ is generated across the series capacitor by the proper operation of the VSI to maintain the load voltage sinusoidal with constant magnitude.

B. Discrete-Time Model for Predictive Voltage Control

The equivalent circuit of TDVR shown in Fig. 2 is a second-order circuit. In this circuit, the current through the filter inductor and the voltage across the series capacitor are taken as the state variables. The dynamics of this system are given by the following differential equations:

$$\frac{di_f}{dt} = -\frac{R_f}{L_f}i_f + \frac{1}{L_f}v_{se} + \frac{1}{L_f}v_{inv}, \quad (1)$$

$$\frac{dv_{se}}{dt} = -\frac{1}{C_{se}}i_s - \frac{1}{C_{se}}i_f. \quad (2)$$

Considering \$i_f\$ and \$v_{se}\$ as state variables and \$v_{inv}\$ and \$i_s\$ as input variables, the state-space continuous-time equation is given as

$$\dot{x} = Ax + Bz \quad (3)$$

where \$x = [i_f \ v_{se}]^T\$ and \$z = [v_{inv} \ i_s]^T\$. Also, in (3)

$$A = \begin{bmatrix} -R_f/L_f & 1/L_f \\ -1/C_{se} & 0 \end{bmatrix} \quad B = \begin{bmatrix} 1/L_f & 0 \\ 0 & -1/C_{se} \end{bmatrix}. \quad (4)$$

The discrete-time state-space form of (3) at the \$(k+1)\$th sampling instant with a sampling time of \$T_d\$ is given as follows:

$$x(k+1) = Gx(k) + Hz(k) \quad (5)$$

where \$G\$ and \$H\$ are computed as

$$G = \begin{bmatrix} g_{11} & g_{12} \\ g_{21} & g_{22} \end{bmatrix} = e^{AT_d} \approx I + AT_d + \frac{A^2 T_d^2}{2} \approx \begin{bmatrix} 1 - \frac{R_f T_d}{L_f} - \frac{T_d^2}{2L_f} \left[\frac{1}{C_{se}} - \frac{R_f^2}{L_f} \right] & -\frac{T_d}{L_f} + \frac{R_f T_d^2}{2L_f^2} \\ \frac{T_d}{C_{se}} - \frac{T_d^2 R_f}{2L_f C_{se}} & 1 - \frac{T_d^2}{2L_f C_{se}} \end{bmatrix} \quad (6)$$

$$H = \begin{bmatrix} h_{11} & h_{12} \\ h_{21} & h_{22} \end{bmatrix} = \int_0^{T_d} e^{A\lambda} Bd\lambda \approx \int_0^{T_d} (I + A\lambda)Bd\lambda \approx \begin{bmatrix} \frac{T_d^2}{2L_f C_{se}} & \frac{V_{dc}}{L_f} \left(T_d - \frac{R_f T_d^2}{L_f} \right) \\ -\frac{T_d}{C_{se}} & \frac{T_d^2 V_{dc}}{2L_f C_{se}} \end{bmatrix}. \quad (7)$$

Finally, the dynamics of the considered system in the discrete-time state-space domain are given as

$$i_f(k+1) = g_{11}i_f(k) + g_{12}v_{se}(k) + h_{11}v_{inv}(k) + h_{12}i_s(k) \quad (8)$$

$$v_{se}(k+1) = g_{21}i_f(k) + g_{22}v_{se}(k) + h_{21}v_{inv}(k) + h_{22}i_s(k). \quad (9)$$

C. Selection of Cost Function and Minimization

The predictive voltage control scheme aims to operate VSI such that the load voltage is maintained constant and sinusoidal at all operating conditions. Therefore, the error between the reference injected voltage by the series capacitor and actual injected voltage should be minimized. In the literature, different cost functions based on the control criterion such as active and reactive power control, minimization of switching frequency, dc-link voltage balancing, etc., have been used [14]. In this paper, a cost function of the square of the voltage error between the predicted and the actual series capacitor is considered. It is given as follows:

$$e = [v_{se}^*(k+1) - v_{se}(k+1)]^2. \quad (10)$$

Replacing the predicted voltage of the series capacitor from (8) into (9)

$$e = [v_{se}^*(k+1) - g_{21}i_f(k) - g_{22}v_{se}(k) - h_{21}v_{inv}(k) - h_{22}i_s(k)]^2. \quad (11)$$

While deriving the discrete-time model of the system, it was assumed that the sensed signals remain constant during two subsequent sampling instants. Therefore, the differentiation of the above equation with respect to VSI voltage is given as

$$2[v_{se}^*(k+1) - g_{21}i_f(k) - g_{22}v_{se}(k) - h_{21}v_{inv}(k) - h_{22}i_s(k)] \frac{dv_{se}^*(k+1)}{dv_{inv}(k)} = 0. \quad (12)$$

Solving (11), we obtain

$$v_{se}^*(k+1) - g_{21}i_f(k) - g_{22}v_{se}(k) - h_{21}v_{inv}(k) - h_{22}i_s(k) = 0. \quad (13)$$

From (12), the predictive voltage control law required to achieve a predefined voltage at the load terminal is given as follows:

$$v_{inv}^*(k) = \frac{v_{se}^*(k+1) - g_{21}i_f(k) - g_{22}v_{se}(k) - h_{22}i_s(k)}{h_{21}}. \quad (14)$$

In the above equation, it is observed that the predictive voltage control law includes the future value of the reference injected voltage \$v_{se}^*(k+1)\$. At the \$k\$th sampling instant, its value will not be known. For achieving satisfactory performance, the value of \$v_{se}^*(k+1)\$ needs to be predicted. It is done using present and past values of the reference voltages, also called the extrapolation process. In the following, the second-order extrapolation used for the prediction of \$v_{se}^*(k+1)\$ is given:

$$v_{se}^*(k+1) = 3v_{se}^*(k) - 3v_{se}^*(k-1) + v_{se}^*(k-2). \quad (15)$$

The second-order extrapolation, as given in (15), is appropriate for a wide frequency range and provides satisfactory

compensation performance [21]. However, in case of significant noise or switching ripple content in the point of common coupling (PCC) voltage, the second-order extrapolation may not provide satisfactory compensation performance. In that scenario, a discrete-time filter can be used with the cost function to improve the controller performance [15].

Once the future reference load voltage value is predicted using (14), the reference voltage control law as given in (13) is implemented to maintain the load voltage at the reference value [14].

D. Generation of Reference Voltages for Series Capacitors

The series capacitor of the TDVR is connected between the PCC and load point. The main objective of the TDVR is to inject three-phase voltages such that the load voltages remain balanced and sinusoidal with a constant magnitude even during voltage disturbances. Let the three-phase balanced sinusoidal reference voltages, to be maintained at the load terminal, be given as follows:

$$\begin{aligned} v_{la}^* &= \sqrt{2}V_l^* \sin(2\pi ft - \delta) \\ v_{lb}^* &= \sqrt{2}V_l^* \sin(2\pi ft - 2\pi/3 - \delta) \\ v_{lc}^* &= \sqrt{2}V_l^* \sin(2\pi ft + 2\pi/3 - \delta) \end{aligned} \quad (15)$$

where V_l^* is the reference load voltage magnitude (it is taken as the nominal voltage, i.e., 1.0 p.u. in this paper). Also, the term f corresponds to the supply frequency. A software phase lock loop described in [22] is used for synchronization. The angle δ is the load angle which is used to maintain the power balance at the load point in addition to maintaining the dc-bus voltage constant. It is computed using a proportional-integral (PI) controller which ensures that the load power is taken from the source by maintaining the VSI dc-link voltage constant. The load angle is computed using the following PI controller [9]:

$$\delta = K_p e + K_i \int e dt \quad (16)$$

where e is the error between the reference and actual dc-link voltages. Also, the proportional and integral gains of the controller are K_p and K_i , respectively.

Let v_{ta} , v_{tb} , and v_{tc} be three-phase PCC voltages. Also, the voltages v_{sea}^* , v_{seb}^* , and v_{sec}^* are the reference injected voltages of the series capacitor in phases a , b , and c , respectively. The TDVR injects voltage in series with the line for any deviation in the supply voltage. Hence, injected voltages will be the difference between the instantaneous reference load and PCC voltages. These voltages are given as follows:

$$\begin{bmatrix} v_{sea}^* \\ v_{seb}^* \\ v_{sec}^* \end{bmatrix} = \begin{bmatrix} v_{la}^* \\ v_{lb}^* \\ v_{lc}^* \end{bmatrix} - \begin{bmatrix} v_{ta} \\ v_{tb} \\ v_{tc} \end{bmatrix}.$$

III. SIMULATION RESULTS

The performance of the predictive voltage control scheme for the system given in Fig. 1 is tested in PSCAD software. A

TABLE I
SYSTEM PARAMETERS

System quantities	Values
Source voltage	230 V rms line to neutral, 50 Hz
Feeder parameters	$R_s = 0.2 \Omega$, $L_s = 0.5 \text{ mH}$
Linear load	$Z_{la} = 60 + j62.8 \Omega$, $Z_{lb} = 40 + j78.5 \Omega$, $Z_{lc} = 50 + j50.24 \Omega$
RL type nonlinear load	Three-phase diode-rectifier load $R_{nl} = 50 \Omega$, $L_{nl} = 150 \text{ mH}$
RC type nonlinear load	Three-phase diode-rectifier load $R_{nl} = 50 \Omega$, $C_{nl} = 1000 \mu\text{F}$
TDVR parameters	$V_{dc} = 600 \text{ V}$, $C_{dc} = 2500 \mu\text{F}$, $L_f = 10 \text{ mH}$, $R_f = 0.5 \Omega$
PI gains	$K_p = 6 \times 10^{-6}$, $K_i = 1 \times 10^{-5}$
Sampling frequency	20 kHz

source voltage of 230 V (rms) is considered, and the TDVR reference voltage is also set at 230 V (rms). The sampling frequency is set to 20 kHz (having a sampling time of 50 μs) which is easily achievable in the modern DSP controller used for practical implementations. The system parameters are given in Table I.

The value of the filter inductor needs to be chosen based on criterion such as switching frequency, harmonic level, and filter size [2], [4]. A small inductor reduces the overall filter size; however, the switching frequency will be high, losses in the inverter will be more, and the load voltage will also have significantly high switching frequency components. With a relatively moderate size filter inductor, the filter size increases, but the switching frequency will be low, inverter losses will reduce, and the load voltage will have lesser switching frequency components. Taking these considerations into account, the value of the filter inductor should be chosen as a tradeoff between the constraints like inverter switching frequency, harmonic level in the load voltage, and size of the filter [2], [4].

Initially, a 5-mH inductor is chosen for filter applications. With this filter, the performance of TDVR for a voltage sag of 30% is shown in Fig. 3. In this case, it can be seen that the load voltage is maintained constant and sinusoidal throughout the operation. This confirms the effectiveness of the proposed scheme. However, the load voltage contains a significant switching frequency component along with having a switching frequency of 6.8 kHz.

To reduce the switching frequency as well as the harmonic level in load voltage, a moderate size inductor of 10 mH is used as filter inductance. First, linear reactive and *RL*-type nonlinear loads are considered. Simulation results for a 30% voltage sag are shown in Fig. 4. The figure includes the source voltage (v_s) and load voltage (v_l) before, during, and after the sag. With the average switching frequency of 4.2 kHz, a sinusoidal voltage with a total harmonic distortion (THD) of 1.2% is maintained at the load point. The result confirms that the load voltage waveform has significantly lower switching frequency component and the VSI switching frequency is significantly reduced as compared to the result with the 5-mH filter inductance. Also, the load voltage waveform is smooth during voltage disturbance (i.e., during normal to sag and vice versa). Furthermore, Fig. 5 shows the performance of the predictive control scheme during a voltage swell of 30%. Again, the load voltage is sinusoidal

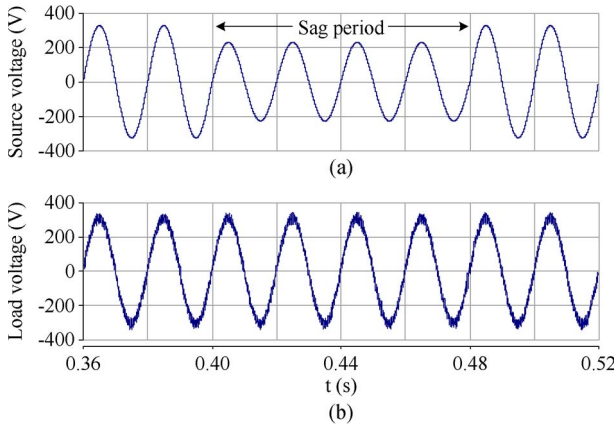


Fig. 3. Simulation waveforms under voltage sag with 5-mH filter inductance. (a) Source voltage. (b) Load voltage.

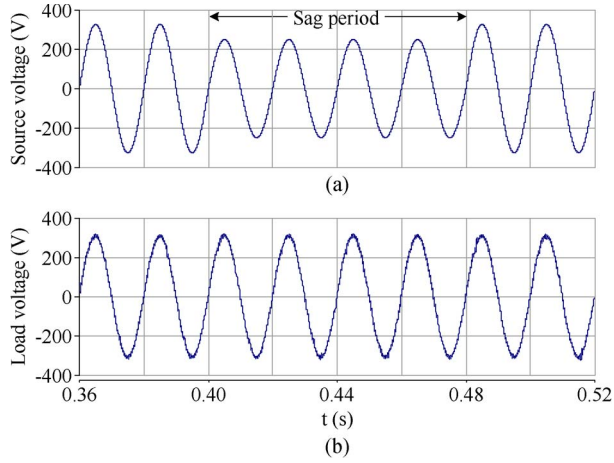


Fig. 4. Simulation waveforms under voltage sag. (a) Source voltage. (b) Load voltage.

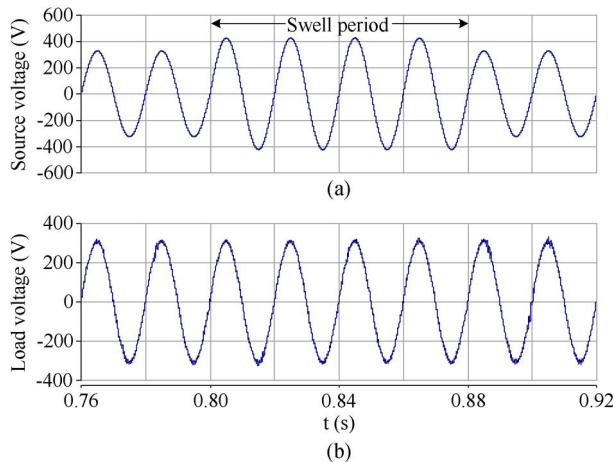


Fig. 5. Simulation waveforms under voltage swell. (a) Source voltage. (b) Load voltage.

and maintained constant throughout the operation without any transients.

The performance of the predictive controller is also tested with the RC -type nonlinear load, and the corresponding results are shown in Fig. 6. The load current in this case is highly distorted. A voltage sag of 30% is created for four cycles.

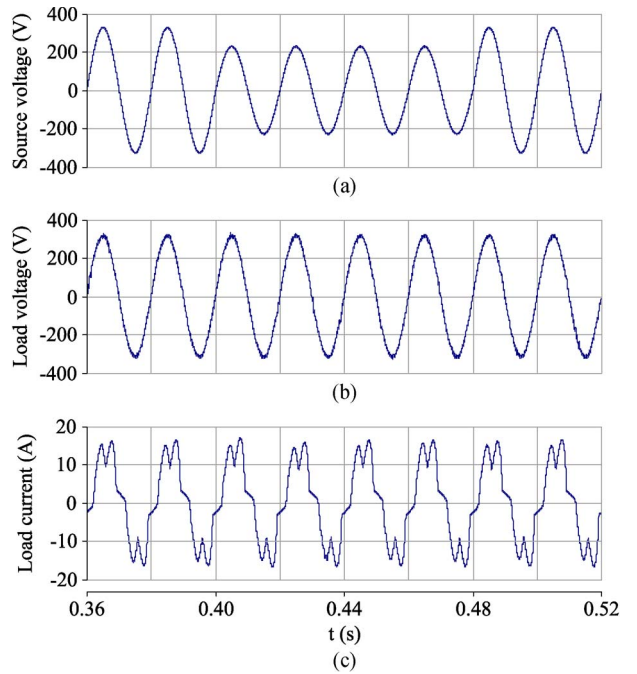


Fig. 6. Simulation waveforms under voltage sag with RC -type nonlinear load. (a) Source voltage. (b) Load voltage. (c) Load current.

The load voltage is maintained at its reference value throughout the operation, whereas the load current is drawn as per the requirement. The waveforms confirm that the predictive control scheme works effectively even with highly nonlinear RC -type load.

IV. EXPERIMENTAL RESULTS

The predictive voltage control scheme is implemented on a TMS320F2812 DSP to control a reduced scale experimental setup with a source voltage of 50 V (rms). The power circuit of TDVR consists of a SEMIKRON-made VSI, an output filter, Hall effect voltage and current transducers, signal conditioning circuit, and a host computer with a code composer studio. The reference load voltage magnitude is set at 50 V. The DSP takes 30 μ s to execute the algorithm, and therefore, a sampling time of 50 μ s is set. The experiments are conducted only for reactive and RL -type nonlinear load. Except for the source voltage, all the parameters of test the system are the same as given in Table I.

Fig. 7 shows the performance of the predictive controller during voltage sag. The voltage sag is created using a programmable ac power supply which reduces the source voltage by 30% for four cycles. Moreover, the load voltage is maintained constant, sinusoidal, and with negligible ripple. Furthermore, the compensation performance of TDVR during voltage swell is shown in Fig. 8, where the source voltage is increased by 30%. The scheme provides fast voltage regulation by maintaining the load voltage at the reference value throughout the operation.

The simulation and experimental waveforms validate that the predictive voltage control scheme tracks the reference voltage effectively while maintaining load voltages sinusoidal under different operating conditions.

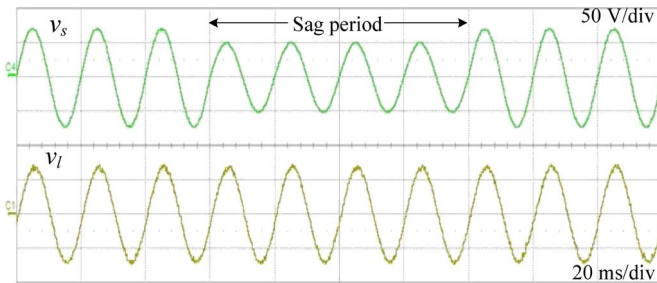


Fig. 7. Experimental waveforms of source voltage (v_s) and load voltage (v_l) during voltage sag.

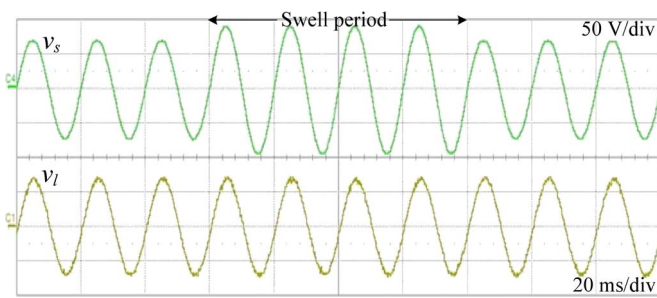


Fig. 8. Experimental waveforms of source voltage (v_s) and load voltage (v_l) during voltage swell.

V. CONCLUSION

The predictive voltage control scheme suitable for the operation of TDVR has been presented in this paper. This scheme provides good voltage tracking and dynamic performance without utilizing any linear controller or modulation technique. The scheme can be easily realized by implementing the discrete-time model of the system in modern DSP processor. The simulation and experimental results confirm the usefulness of this scheme.

REFERENCES

- [1] M. Bollen, *Understanding Power Quality Problems*. Piscataway, NJ, USA: IEEE Press, 2000.
- [2] K. Karanki, G. Gedda, M. K. Mishra, and B. Kumar, "A modified three-phase four-wire UPQC topology with reduced dc-link voltage rating," *IEEE Trans. Ind. Electron.*, vol. 60, no. 9, pp. 3555–3566, Sep. 2013.
- [3] M. Moradlou and H. Karshenas, "Design strategy for optimum rating selection of interline DVR," *IEEE Trans. Power Del.*, vol. 26, no. 1, pp. 242–249, Jan. 2011.
- [4] S. Sasitharan and M. K. Mishra, "Constant switching frequency band controller for dynamic voltage restorer," *IET Power Electron.*, vol. 3, no. 5, pp. 657–667, Sep. 2010.
- [5] F. Badrkhani Ajaei, S. Afsharnia, A. Kahrobaeian, and S. Farhangi, "A fast and effective control scheme for the dynamic voltage restorer," *IEEE Trans. Power Del.*, vol. 26, no. 4, pp. 2398–2406, Oct. 2011.
- [6] P. Kanjiya, B. Singh, A. Chandra, and K. Al-Haddad, "'SRF theory revisited' to control self-supported Dynamic Voltage Restorer (DVR) for unbalanced and nonlinear loads," *IEEE Trans. Ind. Appl.*, vol. 49, no. 5, pp. 2330–2340, Sep./Oct. 2013.
- [7] W. Santos *et al.*, "The transformerless single-phase universal active power filter for harmonic and reactive power compensation," *IEEE Trans. Power Electron.*, vol. 29, no. 7, pp. 3563–3572, Jul. 2014.
- [8] B. H. Li, S. Choi, and D. Vilathgamuwa, "Transformerless dynamic voltage restorer," *Proc. Inst. Elect. Elec.—Gen. Transmiss. Distrib.*, vol. 149, no. 3, pp. 263–273, May 2002.
- [9] A. Ghosh and G. F. Ledwich, *Power Quality Enhancement Using Custom Power Devices*. Boston, MA, USA: Kluwer, 2002.
- [10] C. Rojas *et al.*, "Predictive torque and flux control without weighting factors," *IEEE Trans. Ind. Electron.*, vol. 60, no. 2, pp. 681–690, Feb. 2013.
- [11] Z. Song, C. Xia, and T. Liu, "Predictive current control of three-phase grid-connected converters with constant switching frequency for wind energy systems," *IEEE Trans. Ind. Electron.*, vol. 60, no. 6, pp. 2451–2464, Jun. 2013.
- [12] R. Portillo, S. Vazquez, J. Leon, M. Prats, and L. Franquelo, "Model based adaptive direct power control for three-level NPC converters," *IEEE Trans. Ind. Informat.*, vol. 9, no. 2, pp. 1148–1157, May 2013.
- [13] J. Moreno, J. Huerta, R. Gil, and S. Gonzalez, "A robust predictive current control for three-phase grid-connected inverters," *IEEE Trans. Ind. Electron.*, vol. 56, no. 6, pp. 1993–2004, Jun. 2009.
- [14] P. Cortes, M. Kazmierkowski, R. Kennel, D. Quevedo, and J. Rodriguez, "Predictive control in power electronics and drives," *IEEE Trans. Ind. Electron.*, vol. 55, no. 12, pp. 4312–4324, Dec. 2008.
- [15] P. Cortes, J. Rodriguez, D. Quevedo, and C. Silva, "Predictive current control strategy with imposed load current spectrum," *IEEE Trans. Power Electron.*, vol. 23, no. 2, pp. 612–618, Mar. 2008.
- [16] E. Wu and P. Lehn, "Digital current control of a voltage source converter with active damping of LCL resonance," *IEEE Trans. Power Electron.*, vol. 21, no. 5, pp. 1364–1373, Sep. 2006.
- [17] L. Hang, S. Liu, G. Yan, B. Qu, and Z.-yu Lu, "An improved deadbeat scheme with fuzzy controller for the grid-side three-phase PWM boost rectifier," *IEEE Trans. Power Electron.*, vol. 26, no. 4, pp. 1184–1191, Apr. 2011.
- [18] O. Kukrer and H. Komurcugil, "Deadbeat control method for single phase UPS inverters with compensation of computation delay," *Proc. Inst. Elect. Eng.—Elect. Power Appl.*, vol. 146, no. 1, pp. 123–128, Jan. 1999.
- [19] J. Holtz *et al.*, "Design of fast and robust current regulators for high-power drives based on complex state variables," *IEEE Trans. Ind. Appl.*, vol. 40, no. 5, pp. 1388–1397, Sep./Oct. 2004.
- [20] O. Kukrer, "Discrete-time current control of voltage-fed three-phase PWM inverters," *IEEE Trans. Power Electron.*, vol. 11, no. 2, pp. 260–269, Mar. 1996.
- [21] J. Rodriguez *et al.*, "Predictive current control of a voltage source inverter," *IEEE Trans. Ind. Electron.*, vol. 54, no. 1, pp. 495–503, Feb. 2007.
- [22] C. Zhan *et al.*, "Software phase-locked loop applied to Dynamic Voltage Restorer (DVR)," in *Proc. IEEE Power Eng. Soc. Winter Meet.*, 2001, vol. 3, pp. 1033–1038.



Chandan Kumar (S'13) received the B.Sc. degree in electrical engineering from Muzaffarpur Institute of Technology, Muzaffarpur, India, in 2009 and the M.Tech. degree in electrical engineering from the National Institute of Technology, Trichy, India, in 2011.

He is currently a Research Student with the Department of Electrical Engineering, Indian Institute of Technology Madras, Chennai, India. His research interests include active power filters, power quality, and renewable energy.



Mahesh K. Mishra (S'00–M'02–SM'10) received the B.Tech. degree in electrical engineering from the College of Technology, Pantnagar, India, in 1991, the M.E. degree in electrical engineering from the University of Roorkee, Roorkee, India, in 1993, and the Ph.D. degree in electrical engineering from the Indian Institute of Technology, Kanpur, India, in 2002.

He has teaching and research experience of about 23 years. For about ten years, he was with the Electrical Engineering Department, Visvesvaraya National Institute of Technology, Nagpur, India. He is currently a Professor in the Electrical Engineering Department, Indian Institute of Technology Madras, Chennai, India. His research interests are in the areas of power distribution systems, power electronics, microgrids, and renewable energy systems.

Dr. Mishra is a Life Member of the Indian Society of Technical Education.